Prospects of determination of reheating temperature after inflation by DECIGO

Sachiko Kuroyanagi[1], Kazunori Nakayama[2], and Jun'ichi Yokoyama[3,4]
[1]*Department of Physics, Tokyo University of Science, Kagrazaka, Japan*
[2]*Department of Physics, Graduate School of Science, The University of Tokyo, Tokyo 113-0033, Japan*
[3]*Research Center for the Early Universe (RESCEU), Graduate School of Science, The University of Tokyo, Tokyo 113-0033, Japan*
[4]*Kavli Institute for the Physics and Mathematics of the Universe (Kavli IPMU), WPI, TODIAS, The University of Tokyo, Kashiwa, Japan*

(Dated: December 12, 2014)

If the tensor-to-scalar ratio r of cosmological perturbations takes a large value $r \sim 0.1$, which may be inferred by recent BICEP2 result, we can hope to determine thermal history, in particular, the reheating temperature, T_R, after inflation by space-based laser interferometers. It is shown that upgraded and upshifted versions of DECIGO may be able to determine T_R if it lies in the range $6 \times 10^6 < T_R < 5 \times 10^7$GeV and $3 \times 10^7 < T_R < 2 \times 10^8$GeV, respectively. Although these ranges include predictions of some currently plausible inflation models, since each specification can probe T_R of at most a decade range, we should determine the specifications of DECIGO with full account of constraints on inflation models to be obtained by near-future observations of temperature anisotropy and B-model polarization of the cosmic microwave background radiation.

arXiv:1410.6618v2 [astro-ph.CO] 11 Dec 2014

After more than three decades from its original proposal [1, 2], the inflationary cosmology is now confronting and passing a number of observational tests. Among its generic predictions, the spatial flatness and generation of almost scale-invariant spectrum of curvature perturbations [3] were first confirmed by precise measurements of the cosmic microwave background radiation (CMB) by WMAP [4, 5] and are now being updated by Planck [6, 7]. The Gaussian nature of these fluctuations has also been further confirmed recently by Planck [8].

In March 2014, the BICEP2 collaboration [9] reported detection of the B-mode polarization of CMB over a fairly wide range of angular multipoles from $\ell \simeq 40$ to 350. The higher multipole range can be explained by gravitational lensing while the smaller multipoles are interpreted as owing to the long-wave gravitational waves of primordial origin, most likely from the tensor perturbations generated quantum mechanically during inflationary expansion stage in the early Universe [10]. If what they measured had not been contaminated by foregrounds, it would correspond to the amplitude of the tensor-to-scalar ratio as $r = 0.20^{+0.07}_{-0.05}$ [9]. Note that r is related with the energy scale of inflation as $V = (3.2 \times 10^{16}\text{GeV})^4 r$.

This value, on the other hand, is larger than that expected by the constraints imposed by WMAP [5] and Planck [7] in terms of temperature anisotropy and E-mode polarization, because they reported 95% upper bounds on r as $r < 0.13$ and 0.11, respectively, and that the likelihood contours in (n_s, r) plane preferred the tensor-to-scalar ratio significantly smaller than 0.1. As a result, models predicting tiny values of r such as $r \sim 10^{-3}$ had been investigated extensively including the curvature square inflation [2] and the original Higgs inflation model [11], which occupy the central region of the likelihood contours. These models would be ruled out if large tensor perturbation would be observationally established [1].

After the original announcement of BICEP2, several analyses of the effects of dust contamination have been done, and it has been pointed out that they may be so large that the observed B-mode polarization may be entirely due to the dust foreground [15] and we only have an upper bound on r.

In any event, the BICEP2 observation has reminded us the lesson that the truth may not lie in the center of the likelihood contour and we should remain open-minded until the final result is established. Hence here we consider the case with r close to its observational upper bound $r \sim 0.1$. The most plausible feature of a relatively large value of r is that direct observation of tensor perturbations becomes more feasible by future space-based laser interferometers such as DECIGO [16], which also allow us to extract useful information on the thermal history after inflation [17]. For example, information on reheating is imprinted in the gravitational wave spectrum in the frequencies corresponding to the energy scale of reheating. Thus, the targeting frequency of the experiment is a key for determining reheating temperature and would be better to be adjusted once we obtain a hint about reheating from either cosmology or

[1] Even in such a case the Higgs field in the Standard Model could be an inflaton, because newer Higgs inflation models such as Higgs G-inflation [12] or running kinetic inflation [13] could work well to accommodate large enough r as summarized in [14].

particle physics. In this paper, we discuss the range of the reheating temperature which can be determined by DECIGO and its upgraded and ultimate versions based on the updated sensitivity curves than that used in [18]. We also consider a specification whose sensitivity is shifted to higher frequencies and see how the range of reheating temperature changes.

Specifically, we first consider the chaotic inflation model [19] driven by a massive scalar field for which sensible particle physics models exist [20]. This model predicts tensor-to-scalar ratio $r = 0.13 \sim 0.16$ at $N = 60 \sim 50$ e-folds before the end of inflation, and so fits the lower tail of the BICEP2 result well, which may also be allowed by WMAP and Planck observations, if not preferred. Just in case a significant fraction of the BICEP2 result is due to the dust foregrounds, we also consider a natural inflation model with the symmetry breaking scale $v = 7M_{Pl}$, which predicts $r = 0.07 \sim 0.09$, for comparison [21]. Here M_{Pl} is the reduced Planck scale.

As usual, we incorporate tensor perturbations h_{ij} to spatially flat Friedmann-Lemaitre-Robertson-Walker (FLRW) spacetime as

$$ds^2 = -dt^2 + a^2(t)(\delta_{ij} + h_{ij})dx^i dx^j = a^2(\tau)[-d\tau^2 + (\delta_{ij} + h_{ij})dx^i dx^j], \tag{1}$$

where $a(t)$ is the scale factor, τ is the conformal time, and indices i, j run from 1 to 3. We impose transverse-traceless condition on h_{ij}, $\partial_i h_{ij} = 0 = h^i_i$.

We perform Fourier expansion as

$$h_{ij}(t, \boldsymbol{x}) = \sum_{\lambda=+,\times} \int \frac{d^3k}{(2\pi)^{3/2}} \epsilon^\lambda_{ij}(\boldsymbol{k}) h^\lambda_{\boldsymbol{k}}(t) e^{i\boldsymbol{k}\cdot\boldsymbol{x}}, \tag{2}$$

where the polarization tensor ϵ^λ_{ij} $(\lambda = +, \times)$ is normalized as $\sum_{i,j} \epsilon^\lambda_{ij} \epsilon^{*\lambda'}_{ij} = 2\delta^{\lambda\lambda'}$.

Since each polarization mode satisfies

$$\ddot{h}^\lambda_{\boldsymbol{k}}(t) + 3H\dot{h}^\lambda_{\boldsymbol{k}}(t) + \frac{k^2}{a^2(t)} h^\lambda_{\boldsymbol{k}}(t) = 0, \tag{3}$$

which is the same as the Klein-Gordon equation for a massless minimally coupled scalar field, we can quantize it during inflaton using the conventional wisdom of quantum field theory in curved spacetime [10]. Here H is the Hubble parameter and a dot denotes time derivative. As a result, we find a nearly scale-invariant long wave fluctuation as an initial condition [10] with the amplitude

$$\Delta^2_h(k) = \langle h_{ij} h^{ij}(k) \rangle = 64\pi G \left(\frac{H(t_k)}{2\pi} \right)^2, \tag{4}$$

where $H(t_k)$ is the Hubble parameter during inflation when k-mode left the horizon, and the prefactor is determined by the canonical quantization based on the Einstein action. This weak wavenumber dependence may be incorporated by Taylor expansion with respect to $\ln(k/k_*)$ as

$$\Delta^2_h(k) = \Delta^2_h(k_*) \exp\left[n_T(k_*) \ln\frac{k}{k_*} + \frac{1}{2!}\alpha_T(k_*) \left(\ln\frac{k}{k_*} \right)^2 + \frac{1}{3!}\beta_T(k_*) \left(\ln\frac{k}{k_{\rm piv}} \right)^3 + \cdots \right]. \tag{5}$$

Here k_* is a pivot scale where the tensor-to-scalar ratio $r(k_*)$ is formally defined by

$$r \equiv \frac{\Delta^2_h(k_*)}{\Delta^2_s(k_*)}, \tag{6}$$

with $\Delta^2_s(k_*)$ being the square amplitude of curvature perturbation at the pivot scale k_*. Planck takes $k_* = 0.002\mathrm{Mpc}^{-1}$ [6]. In a single-field slow-roll inflation model with a potential $V[\phi]$, coefficients in (5) as well as r are given by the slow-roll parameters,

$$\epsilon_V[\phi] \equiv \frac{M^2_{\rm Pl}}{2} \left(\frac{V'[\phi]}{V[\phi]} \right)^2, \quad \eta_V[\phi] \equiv M^2_{\rm Pl} \frac{V''[\phi]}{V[\phi]}, \quad \xi_V[\phi] \equiv M^4_{\rm Pl} \frac{V'[\phi]V'''[\phi]}{V[\phi]^2}, \tag{7}$$

as

$$r = 16\epsilon_V, \quad n_T = -2\epsilon_V, \quad \alpha_T(k) = -4\epsilon_V(2\epsilon_V - \eta_V), \quad \beta_T(k) = -4\epsilon_V(16\epsilon_V^2 + 2\eta_V^2 - 14\epsilon_V\eta_V + \xi_V^2), \tag{8}$$

respectively. In order to obtain the accurate amplitude of gravitational waves at the direct detection scale $\sim$ 1Hz, (5) is insufficient and we must continue Taylor expansion up to sixth order [22]. Then it agrees with the full numerical solution of the mode equation for the models we consider here [23, 24]. In this paper, we use the sixth-order Taylor expansion [22] in order to save the computation time.

The field equations for ϕ are given as

$$\ddot{\phi} + 3H\dot{\phi} + V'[\phi] = 0, \quad \left(\frac{\dot{a}}{a}\right)^2 = \frac{\rho_\phi}{3M_{\rm Pl}^2}, \quad \rho_\phi = \frac{1}{2}\dot{\phi}^2 + V[\phi], \tag{9}$$

during inflation, and

$$\ddot{\phi} + (3H+\Gamma)\dot{\phi} + V'[\phi] = 0, \quad \frac{d\rho_r}{dt} = -4H\rho_r + \Gamma\dot{\phi}^2, \quad \left(\frac{\dot{a}}{a}\right)^2 = \frac{1}{3M_{\rm Pl}^2}(\rho_\phi + \rho_r), \tag{10}$$

in the field oscillation regime where ρ_r is the radiation energy density and Γ is the decay rate of the inflaton that determines the reheating temperature. In the mid and late field oscillation regime when the mass term dominates the potential, the scalar field equation is replaced by

$$\frac{d\rho_\phi}{dt} = -(3H+\Gamma)\rho_\phi. \tag{11}$$

During slow roll inflation, $\ddot{\phi}$ and kinetic energy term are negligible and we can find a well known slow-roll analytic solution for the massive chaotic inflation [19] with a quadratic potential

$$V[\phi] = m^2\phi^2/2. \tag{12}$$

We can express the number of e-folds $N \equiv \ln(a_{\rm end}/a)$ as

$$N \cong \frac{1}{M_{\rm Pl}^2}\int_{\phi_{\rm end}}^{\phi}\frac{V[\phi]}{V'[\phi]}d\phi = \frac{\phi^2}{4M_{\rm Pl}^2} - \frac{1}{2}, \quad \phi_{\rm end} = \frac{M_{Pl}}{\sqrt{2}}. \tag{13}$$

Then the slow-roll parameters and r are given in terms of N,

$$\epsilon_V = \eta_V = 2\frac{M_{\rm Pl}^2}{\phi^2} = \frac{1}{2N+1}, \quad r = 16\epsilon_V = \frac{16}{2N+1}. \tag{14}$$

All the higher derivative slow-roll parameters including ξ_V are equal to zero.

From the numerical solution of field equations, we can calculate the number of e-folds of inflation after the pivot scale k_* left the Hubble radius as

$$N_* = 54.4 + \frac{1}{3}\ln\left(\frac{T_R}{10^8{\rm GeV}}\right). \tag{15}$$

From (14) and (15), we can obtain the reheating temperature modulo dilution factor once the tensor-to-scalar ratio is measured as

$$T_R = 1.7\times10^6\exp\left[160\left(\frac{r}{0.15}\right)^{-1}\right]\ {\rm GeV}. \tag{16}$$

Later each mode evolves as

$$h_{\boldsymbol{k}}^\lambda(t) \propto a(t)^{\frac{1-3p}{2p}} J_{\frac{3p-1}{2(1-p)}}\left(\frac{p}{1-p}\frac{k}{a(t)H(t)}\right) = a(\tau)^{\frac{1-3p}{2p}} J_{\frac{3p-1}{2(1-p)}}(k\tau), \tag{17}$$

in a power-law background $a(t) \propto t^p$ with $p < 1$. Here $J_n(x)$ is a Bessel function. Thus the amplitude of $h_{\boldsymbol{k}}^\lambda(t)$ remains constant in the super-horizon regime and it starts to decrease inversely proportional to the scale factor after horizon crossing, so that the energy density of gravitational waves,

$$\rho_{\rm GW} = \frac{1}{64\pi G a^2}\langle(\partial_\tau h_{ij})^2 + (\nabla h_{ij})^2\rangle, \tag{18}$$

decreases in the same way as radiation for modes well inside the horizon.

We define density parameter of gravitational waves of each logarithmic frequency interval as

$$\Omega_{\rm GW}(f,t_0) \equiv \frac{1}{\rho_c}\frac{d\rho_{\rm GW}}{d\ln k} = \frac{1}{12}\left(\frac{k}{a_0H_0}\right)^2 \Delta_h^2(k)T_h^2(f) = \frac{(2\pi f)^2}{12H_0^2}\Delta_h^2(f)T_h^2(f), \tag{19}$$

where $T_h(k)$ is the transfer function given by

$$T_h^2(k) = \Omega_m^2 \frac{g_*(T_{\rm in})}{g_{*0}}\left(\frac{g_{*s0}}{g_*(T_{\rm in})}\right)^{4/3}\frac{9j_1^2(k\tau_0)}{(k\tau_0)^2}T_1^2(x_{\rm eq})T_2^2(x_{\rm R}). \tag{20}$$

Here the subscripts 0 and in refer to the values at the present time τ_0 and at the epoch when k-mode reentered the Hubble radius, respectively. g_* and g_{*s} represent the effective numbers of degrees of freedom for energy and entropy densities with their current values given by $g_{*0} = 3.36$ and $g_{*s0} = 3.90$, respectively. We take $\tau_0 = 2H_0^{-1}$, which is the right expression for matter domination, and incorporate the effect of dark energy by the factor $\Omega_m = 1 - \Omega_{DE}$. In the limit $k\tau_0 \gg 1$ in which we are interested, we can replace the square of the spherical Bessel function by averaging over the period as $\overline{j_1^2(k\tau_0)} \cong (2k\tau_0)^{-2}$. The first transfer function $T_1(x_{\rm eq})$ represents the effect of transition from the radiation to the matter domination [25], while the second one $T_2(x_{\rm R})$ stands for that from the field oscillation regime to the radiation dominated era at the reheating just after inflation [26]. They are explicitly given by [27]

$$T_1^2(x_{\rm eq}) = (1 + 1.41x_{\rm eq} + 3.56x_{\rm eq}^2), \tag{21}$$

with $x_{\rm eq} = k/k_{\rm eq}$ and $k_{\rm eq} \equiv \tau_{\rm eq}^{-1} = 7.1\times10^{-2}\Omega_m h^2\,{\rm Mpc}^{-1}$, and [28]

$$T_2^2(x_{\rm R}) = (1 - 0.22x_{\rm R}^{1.5} + 0.65x_{\rm R}^2)^{-1}, \tag{22}$$

with $x_{\rm R} = k/k_{\rm R}$ and $k_{\rm R} \simeq 1.7\times10^{14}{\rm Mpc}^{-1}(g_{*s}(T_{\rm R})/106.75)^{1/6}(T_{\rm R}/10^7{\rm GeV})$, respectively. Here $k_{\rm R}$ is related with the current frequency

$$f_{\rm R} = \frac{k_{\rm R}}{2\pi a_0} \simeq 0.26{\rm Hz}\left(\frac{g_{*s}(T_{\rm R})}{106.75}\right)^{1/6}\left(\frac{T_{\rm R}}{10^7{\rm GeV}}\right). \tag{23}$$

This is the frequency where the spectrum of stochastic gravitational wave background is bent and the reheating temperature is encoded. The density parameter therefore behaves as $\Omega_{\rm GW}(f,t_0) \propto f^{-2}(f^0)$ for the mode which enters the horizon in the matter (radiation) dominated regime. More generally, for modes entering the horizon when the equation-of-state parameter or the ratio of pressure to energy density was w, its frequency dependence reads

$$\Omega_{\rm GW}(f) \propto f^{\frac{2(3w-1)}{3w+1}}. \tag{24}$$

The above is the case where the Universe evolves adiabatically after reheating at the end of inflation. If there is additional entropy production from a decaying matter component χ like Polonyi [29] or moduli fields [30] which temporarily dominates the cosmic energy density, short-wave gravitational radiation is diluted and $k_{\rm R}$ is modified [17, 26]. In terms of the dilution factor,

$$F = \frac{s(T_\chi)a^3(T_\chi)}{s(T_R)a^3(T_R)}, \tag{25}$$

we find the transfer function in this case as

$$T_h^2(k) = \Omega_m^2 \frac{g_*(T_{\rm in})}{g_{*0}}\left(\frac{g_{*s0}}{g_*(T_{\rm in})}\right)^{4/3}\frac{9j_1^2(k\tau_0)}{(k\tau_0)^2}T_1^2(x_{\rm eq})T_2^2(x_{FR})T_3^2(x_\chi)T_2^2(x_{\chi R}), \tag{26}$$

where [28]

$$T_3^2(x_\chi) = (1 + 0.59x_\chi + 0.65x_\chi^2), \tag{27}$$

and $x_{FR},\ x_\chi$, and $x_{\chi R}$ are given by

$$x_{FR} = \frac{F^{1/3}k}{k_R},\quad x_\chi = \frac{k}{k_\chi},\quad x_{\chi R} = \frac{k}{F^{2/3}k_\chi}, \tag{28}$$

with

$$k_\chi = 1.7\times 10^7\ \mathrm{Mpc}^{-1}\left(\frac{g_{*s}(T_\chi)}{106.75}\right)^{1/6}\left(\frac{T_\chi}{1\ \mathrm{GeV}}\right). \tag{29}$$

The Universe is dominated by χ in the regime modes with $k_\chi < k < F^{2/3}k_\chi$ enter the horizon. For wavenumber $k_{\chi R} < k < k_R$, which corresponds to the mode entering the horizon in the radiation dominated era before χ-domination, the energy density of the gravitational waves is suppressed by the factor $\sim (k_\chi/k_{\chi R})^2 = F^{-4/3}$ [17]. We also note that the frequency where the spectrum bends due to the reheating is modified as

$$f_{FR} = 0.026\ \mathrm{Hz} F^{-1/3}\left(\frac{g_{*s}(T_R)}{106.75}\right)^{1/6}\left(\frac{T_R}{10^6\ \mathrm{GeV}}\right), \tag{30}$$

as is clear from the above discussion. Furthermore in the presence of late-time entropy production (15) and (16) are modified as

$$N_* = 54.4 + \frac{1}{3}\ln\left(\frac{T_R/F}{10^8\mathrm{GeV}}\right), \quad \frac{T_R}{F} = 1.7\times 10^6 \exp\left[160\left(\frac{r}{0.15}\right)^{-1}\right]\ \mathrm{GeV}, \tag{31}$$

respectively.

We analyze the detectability of T_R in terms of the Fisher information matrix approach following [18] (see also [31–33]), and discuss improvements of specifications of DECIGO to increase the measurable range of T_R.

Suppose that the stochastic gravitational wave background $\Omega_{\mathrm{GW}}(f, t_0)$ depends on parameters p_i. Then since its detection is done based on cross correlation of two (or more) detectors, the Fisher matrix element $\mathcal{F}_{ij}$ is determined by their noise power spectra $N_I(f)$ as

$$\mathcal{F}_{ij} = \left(\frac{3H_0^2}{10\pi^2}\right)^2 2\,T_{\mathrm{obs}}\sum_{(I,J)}\int_{f_{\mathrm{cut}}}^{f_{\max}} df \frac{|\gamma_{IJ}(f)|^2 \partial_{p_i}\Omega_{\mathrm{GW}}(f)\partial_{p_j}\Omega_{\mathrm{GW}}(f)}{f^6 N_I(f) N_J(f)},$$

where T_{obs} is observation time and $\gamma_{IJ}(f)$ is the overlap reduction function determined by the survey configuration [34]. Here we take $f_{\mathrm{cut}} = 0.1$Hz unless otherwise stated, below which the signal may be contaminated by noise from cosmological white dwarf binaries [35]. We set $f_{\max} = \infty$, but this choice is largely irrelevant to the final result since the high-frequency range is limited by the noise spectrum as shown in [18].

We consider two sets of Fabry-Perot type DECIGO (FP-DECIGO) each consisting of three satellites with an equilateral triangular configuration. The overlap reduction function is given as

$$\gamma_{IJ}(f) = \frac{5}{8\pi}\int d\boldsymbol{\Omega} e^{i2\pi f \boldsymbol{\Omega}\cdot\Delta\boldsymbol{x}} \sum_{A=+,\times} F_I^A(f,\boldsymbol{\Omega}) F_J^A(f,\boldsymbol{\Omega}), \tag{32}$$

where $\Delta\boldsymbol{x}$ is the separation between the two detectors and $F_I^A(f,\boldsymbol{\Omega})$ is the detector pattern functions. For details, see e.g. [36].

The noise power spectrum consists of three mutually independent major components, namely, laser shot noise, S_{shot}, radiation pressure noise, S_{rad}, and acceleration noise, S_{acc}. The noise spectrum of two sets of identical detectors is given by

$$N_1(f) = N_2(f) = S_{\mathrm{shot}}(f) + S_{\mathrm{rad}}(f) + S_{\mathrm{acc}}(f). \tag{33}$$

As with the ground-based Fabry-Perot type interferometers, they depend on the arm length L, the laser power, P, the laser wavelength, λ, the mirror mass, M, the finesse, $\mathcal{F}$ etc. The shot noise and the radiation pressure noise are given by

$$S_{\mathrm{shot}}^{1/2}(f) = \frac{\sqrt{\hbar\pi c\lambda}}{4\mathcal{F}L\sqrt{\tilde{P}}}\left[1+\left(\frac{f}{f_c}\right)^2\right]^{1/2}, \tag{34}$$

$$S_{\mathrm{rad}}^{1/2}(f) = \frac{16\mathcal{F}}{(2\pi f)^2 ML}\sqrt{\frac{\hbar P}{\pi\lambda c}}\left[1+\left(\frac{f}{f_c}\right)^2\right]^{-1/2}, \tag{35}$$

respectively, where c and $\hbar$ are explicitly shown for clarity [37]. Here the cut off frequency f_c is given by

$$f_c = \frac{c}{4L\mathcal{F}}. \tag{36}$$

The finesse, which is the ratio of the resonance separation to the resonance width, and the effective laser output power $\tilde{P}$ are given by the reflectivities of the two mirrors, r_F and r_E, the former referring to the front mirror closer to the laser and the latter the end mirror, and the transmutation rate t_F of the front mirror as

$$\mathcal{F} = \frac{\pi\sqrt{r_F r_E}}{1 - r_F r_E}, \quad \tilde{P} = \left(\frac{t_F^2 r_E}{1 - r_F r_E}\right)^2 P. \tag{37}$$

These parameters are related to L, λ, and the mirror radius R as follows.

$$r_F = r_{Fm} r_G, \quad r_E = r_{Em} r_G, \quad t_F = \sqrt{r_G^2 - r_{Fm}^2}, \quad r_G = 1 - \exp\left(-\frac{2\pi R^2}{\lambda L}\right). \tag{38}$$

Here r_G is the fraction of photons of the ideal Gaussian beam received by the mirror, and r_{Fm} and r_{Em} denote intrinsic reflectivity of each mirror. We take $r_{Fm}^2 = 0.67$ and $r_{Em}^2 = 0.9999$ below.

The acceleration noise, on the other hand, is set to take smaller values than the radiation pressure noise with the effective strain

$$S_{\rm acc}^{1/2}(f) = \frac{16\mathcal{F}}{2(2\pi f)^2 LM}\sqrt{\frac{\hbar P}{\pi\lambda c}}, \tag{39}$$

that is, $S_{\rm rad}^{1/2}(f)/3$ at lower frequencies [38]. Since the maximum measurable reheating temperature is determined by sensitivities at higher frequency, the acceleration noise is actually irrelevant in the subsequent discussion, and the dominant source of detector noise in the relevant frequency range is the shot noise.

The original DECIGO assumes $L = 10^3$km, $P = 10$W, $\lambda = 532$nm, $M = 100$kg, and $R = 0.5$m. With 3 year observations, it will achieve the best sensitivity $\Omega_{\rm GW} = 7.2\times10^{-16}$ at $f = 0.2$Hz, corresponding to the effective strain $h = 2.8\times10^{-25}$. Since this is not sufficient to remove foreground contamination from neutron star binaries [39], upgrade of specifications to achieve three times better sensitivity has been discussed which takes $L = 1.5\times10^3$km, $P = 30$W, $\lambda = 532$nm, $M = 100$kg, and $R = 0.75$m. Then the best sensitivity $\Omega_{\rm GW} = 3.2\times10^{-16}$ is achieved at $f = 0.5$Hz corresponding to $h = 3.0\times10^{-26}$.

In order to keep the same level of sensitivity to $\Omega_{\rm GW}(f)$ at higher frequencies, we must suppress the noise power spectrum $N_I(f)$ in proportion to f^{-3}. To reduce the sensitivity at high frequencies, the shot noise is more important than the radiation pressure noise. To suppress the former, we should decrease the laser wavelength λ or increase the power P, $\mathcal{F}$, and L. However, as we increase $\mathcal{F}L$, f_c becomes smaller and the frequency range of our interest falls above f_c where $S_{\rm shot}(f)$ does not depend on $\mathcal{F}$ nor L. Thus the magnitude of the shot noise can only be controlled by λ and $\tilde{P}$ in the relevant range.

Of course, λ cannot be set arbitrary small. Let us tentatively take a deep UV wavelength $\lambda = 157$nm. Lasers with this wavelength and mirrors with high reflectivity for this band are commercially available now, but stability and high enough power are challenges to be solved by the time when DECIGO will be put into practice in the coming decades. With $\lambda = 157$nm and the laser power $P = 300$W, we could achieve a sensitivity of $\Omega_{\rm GW}$ at $f = 2$Hz similar to that of the upgraded DECIGO at $f = 0.5$Hz. If we should stick to $\lambda = 532$nm, we could obtain the same noise curve by boosting the power to $P \simeq 1$kW since both $S_{\rm shot}(f)$ and $S_{\rm rad}(f)$ depend on the combination P/λ only. In this case, we must take $R = 1.38$m to preserve r_G. Hereafter we shall call this specification the *upshifted* DECIGO and label it as $f_{\rm max} = 2$Hz in the figures to avoid confusion. Figures 1 represent sensitivity of three types of FP-DECIGO in terms of the strain (left panel) and $\Omega_{\rm GW}(f)$ of the stochastic gravitational wave background for 3 years of observation.

Using the above set up, let us first consider the case of chaotic inflation [19] with a quadratic potential (12). From Figs. 2, we find that the maximum value of the reheating temperature that can be determined with $\sigma_{T_R} < T_R$ is $T_R = 5.2\times10^7$GeV for the upgraded DECIGO and $T_R = 2.1\times10^8$GeV for the upshifted DECIGO $f_{\rm max} = 2$Hz, where $\sigma_{T_R}^2$ is the variance of the measurement error. Thus by improving the specification, we can improve the upper limit of the measurable reheating temperature by a factor of 4. We also note that the low frequency cutoff at $f_{\rm cut} = 0.1$Hz due to contamination of white dwarf binaries does not affect the sensitivity to measure T_R as long as we pay attention to the range $\sigma_{T_R} < T_R$. Here we have taken Planck+WP+highL+BAO mean values of cosmological parameters, $\Omega_\Lambda = 0.692$, $\Omega_m h^2 = 0.141$, $h = 0.678$ and $\Delta_s^2 = 2.21\times10^{-9}$ at $k = 0.05{\rm Mpc}^{-1}$ which corresponds to $\Delta_s^2 = 2.51\times10^{-9}$ at our pivot scale $k_* = 0.002{\rm Mpc}^{-1}$ for $n_s = 0.9608$ [6].

Since the combination of λ and P is already ambitious enough, we cannot hope to go further to achieve the desired sensitivity of $\Omega_{\rm GW}$ at even higher frequencies. Because we need the strain sensitivity S_h must be improved

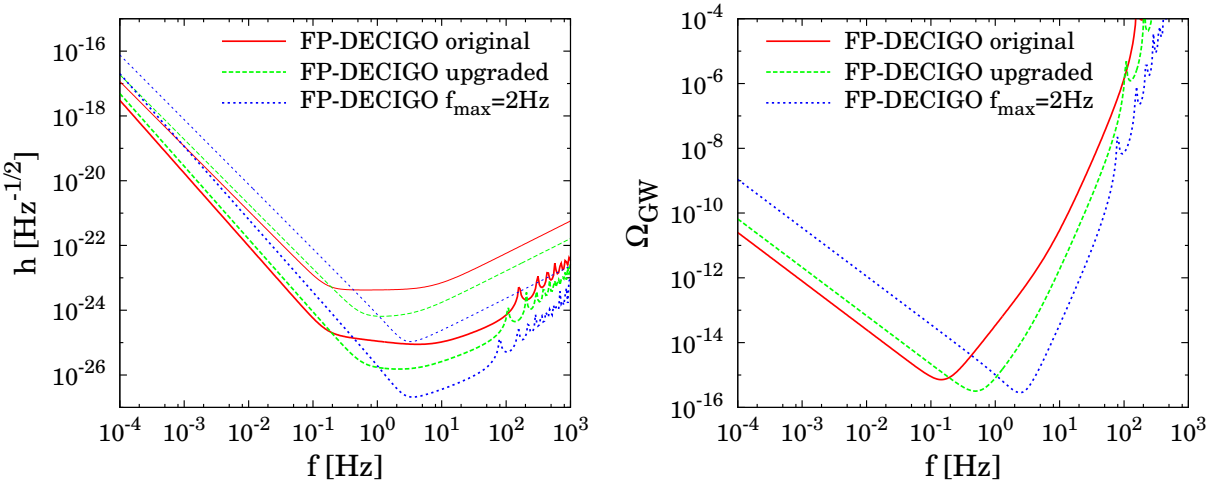

FIG. 1: Noise curves of three types of FP-DECIGO shown in terms of the strain (left panel) and the detectability of $\Omega_{\rm GW}$ for 3 years of observations (right panel). In the left panel, we show the strain sensitivity for one set of detectors (thin curves) and the effective strain sensitivity obtained assuming a 3-year cross-correlation analysis between two sets of detectors (thick curves). In the right panel, we only show the sensitivity curves for the cross-correlation analysis.

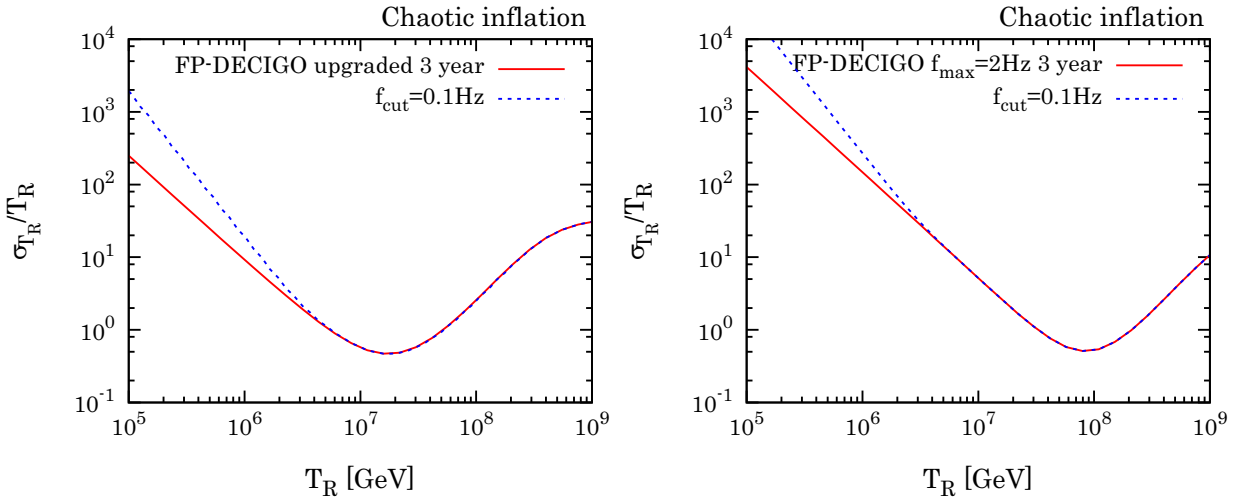

FIG. 2: The marginalized one σ uncertainty in $T_{\rm R}$ as a function of $T_{\rm R}$ for the upgraded FP-DECIGO (left panel) and the upshifted FP-DECIGO with the maximal sensitivity set to $f_{\rm max} = 2$Hz (right panel). Red solid line represents the case with no foreground contamination and blue dotted line shows the case where the range $f < f_{\rm cut} = 0.1$Hz is fully contaminated by binary white dwarfs and cannot be used in the analysis.

in proportion to f^{-3}, it is really difficult to accurately probe almost scale-invariant stochastic gravitational wave background at higher frequencies. Just for completeness, we also consider the ideal case of the ultimate-DECIGO whose noise curve is determined by the quantum limit, with the following specifications: $L = 5 \times 10^5$km, M =100kg, $\lambda = 532$nm, $P = 10$MW, and $R = 3$m, and compare with the above results.

Figure 3 depicts the uncertainty in the measurement of T_R in three specifications of DECIGO. For this particular inflation model one can determine the reheating temperature by using the relation between the amplitude of tensor perturbation and N through (14) and (15) even without observing the spectral bend due to the change of the equation of state during reheating regime. This is why σ_{T_R} saturates at higher T_R for which f_R is beyond the observable range. In practice, we do not know the exact shape of the inflaton potential a priori, hence this saturation should be regarded as an artifact of our analysis using a specific model of inflation from the beginning. Fortunately, however, our results of the measurable ranges of T_R within one σ_{T_R} accuracy are not affected by this as seen in Fig. 3, whose numerical

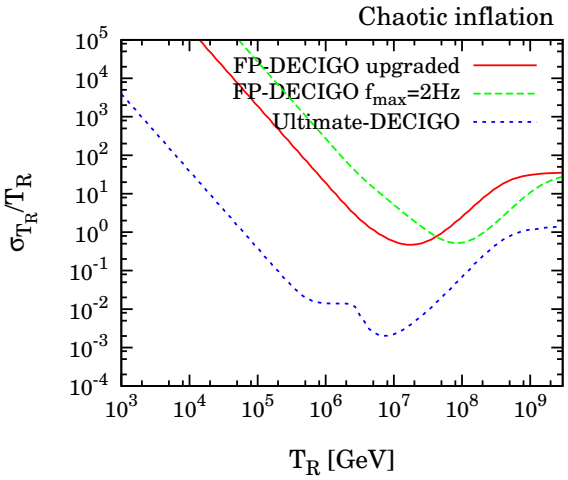

FIG. 3: The marginalized one σ uncertainty in $T_{\rm R}$ as a function of $T_{\rm R}$ for the Ultimate-DECIGO in comparison with the upgraded FP-DECIGO and the upgraded FP-DECIGO with the maximal sensitivity set to $f_{\rm max} = 2$Hz. The low frequency cutoff at $f_{\rm cut} = 0.1$Hz due to contamination of white dwarf binaries is taken into account.

values are shown in Table I.

Chaotic inflation	lower limit	upper limit
FP-DECIGO upgraded	5.6×10^6 GeV	5.2×10^7 GeV
FP-DECIGO $f_{\rm max}$=2Hz	3.3×10^7 GeV	2.1×10^8 GeV
Ultimate-DECIGO	6.2×10^4 GeV	7.0×10^8 GeV

TABLE I: Range of the reheating temperature T_R which can be measured with each specification of DECIGO for massive scalar chaotic inflation.

Next we consider natural inflation [21] with a potential

$$V[\phi] = \Lambda^4 \left[1 - \cos\left(\frac{\phi}{v}\right)\right]. \tag{40}$$

As a specific example, we take $v = 7M_{Pl}$ for which (15) practically applies [24]. In this model, the tensor-to-scalar ratio r corresponding to the number of e-folds N is given by

$$r = \frac{16\nu}{(1+\nu)e^{2\nu N} - 1}, \quad \nu \equiv \frac{M_{Pl}^2}{2v^2}, \tag{41}$$

so we find $r = 0.091$ for $N = 50$ and $r = 0.067$ for $N = 60$. In Figs. 4 and 5, detectability of T_R in this model is depicted. Saturation at higher T_R should again be regarded as an artifact, but it does not affect the one σ_{T_R} range, which is shown in Table II. As is seen there, as far as the upper limit is concerned, the improvement from upgraded FP-DECIGO to the upshifted FP-DECIGO is larger than that from the upshifted specification to ultimate DECIGO, although the lower limit also shifts to a higher value in the former case.

Next we consider the case additional entropy production occurs after reheating stage. Figures 6 depict detectability of gravitational waves in the case F is larger than unity in chaotic inflation. Figures 7 are for the case of the natural inflation with $v = 7M_{Pl}$. As is seen there if F is significant, only ultimate DECIGO can measure the inflationary tensor perturbation.

Let us summarize the results so far. The upgraded DECIGO and the upshifted DECIGO with $f_{\rm max} = 2$Hz can measure the reheating temperature if it takes a value within a factor $\lesssim 10$ from 5×10^6GeV or 3×10^7GeV, respectively. With an appreciable amount of entropy production it would be formidable to detect the tensor perturbation itself, not to mention the detectability of T_R without ultimate DECIGO. Hence let us assume $F = 1$ below and consider the implication of the range of T_R measurable by the upgraded or upshifted DECIGO.

Natural inflation ($v = 7M_{Pl}$)	lower limit	upper limit
FP-DECIGO upgraded	7.0×10^6 GeV	4.2×10^7 GeV
FP-DECIGO $f_{\rm max}$=2Hz	4.0×10^7 GeV	1.8×10^8 GeV
Ultimate-DECIGO	6.9×10^4 GeV	4.6×10^8 GeV

TABLE II: Range of the reheating temperature T_R which can be measured with each specification of DECIGO for natural inflation model with $v = 7M_{Pl}$.

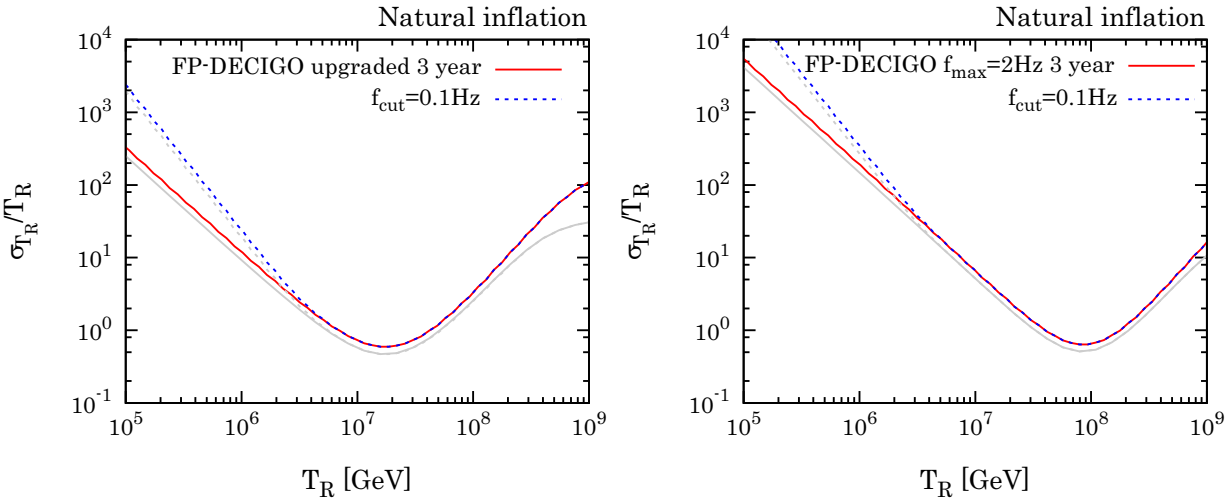

FIG. 4: The marginalized 1σ uncertainty in $T_{\rm R}$ as a function of $T_{\rm R}$ for natural inflation with $v = 7M_{Pl}$. The left panel is for the upgraded FP-DECIGO and the right panel is for the upshifted FP-DECIGO with the maximal sensitivity set to $f = 2$Hz. For comparison, the results for chaotic inflation are also plotted by gray curves.

First of all, a large enough r to make direct detection of inflationary gravitational waves by DECIGO possible means high scale inflation. Thus one may naively think that the reheating temperature is also high, which may not be the case as we argue now. As discussed in [40], high scale inflation means large excursion of the inflaton well beyond M_{Pl}. To stabilize the inflaton potential over such a large field range we need some kind of symmetry, which may also constrain the coupling between the inflaton and matter fields to delay reheating.

The simplest example is natural inflation which is based on the Nambu-Goldstone symmetry. It is natural to suppose that matter coupling with the inflaton is also protected by this symmetry and typical coupling of the inflaton is suppressed by v^{-1}, so that on dimensional grounds the decay rate of the inflaton reads

$$\Gamma \approx g^2 \frac{M^3}{v^2} \approx g^2 \frac{\Lambda^6}{v^5}, \tag{42}$$

where $M \equiv \Lambda^2/v$ is the inflaton mass at the origin [21]. This yields T_R as

$$T_R \approx 5 \times 10^7 \left(\frac{g}{0.1}\right) \text{GeV} \tag{43}$$

for $v = 7M_{Pl}$ where g is a coupling constant.

Chaotic inflation, on the other hand, is also naturally realized introducing a shift symmetry $\phi \to \phi + iC$ with C being a real number [41]. For example, let us take the Kähler potential and superpotential as

$$K = \frac{1}{2}(\phi + \phi^\dagger)^2 + |X|^2 + |H_u|^2 + |H_d|^2, \tag{44}$$

$$W = mX\phi + yXH_uH_d, \tag{45}$$

where ϕ denotes the inflaton superfield whose imaginary component is regarded as the inflaton, X is a singlet chiral superfield and H_u and H_d are up- and down-type Higgs doublets, respectively. In this minimal setup, the reheating

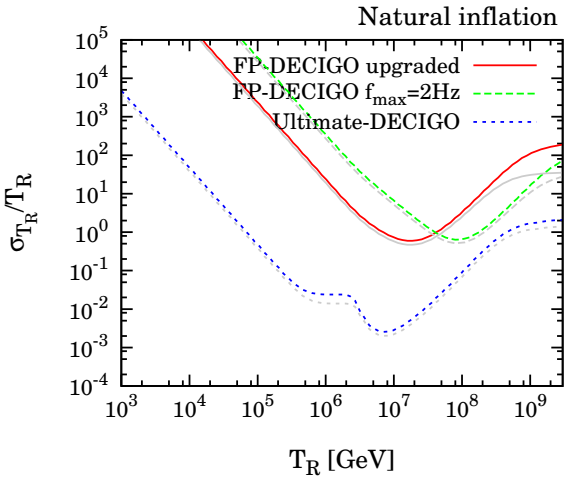

FIG. 5: The comparison of marginalized 1σ uncertainty in $T_{\rm R}$ for natural inflation with $v = 7M_{Pl}$. The low frequency cutoff at $f_{\rm cut} = 0.1$Hz due to contamination of white dwarf binaries is taken into account.

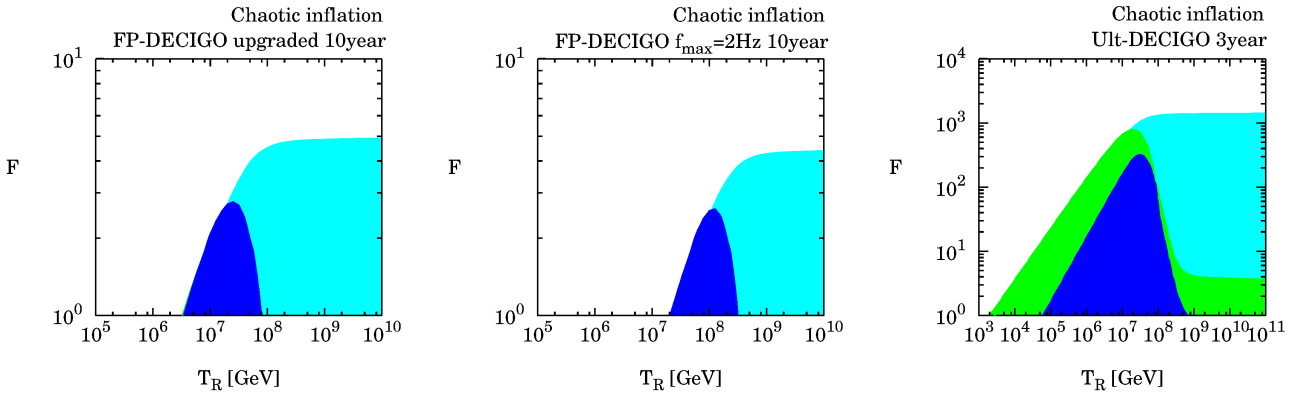

FIG. 6: Light blue region shows the parameter range where stochastic gravitational wave can be detected with S/N>1 for chaotic inflation of massive scalar potential. Thick blue region represents the region the reheating temperature can be measured with an error less than one σ with the cutoff at 0.1Hz, and green region describes the case without the cutoff. For both cases, information from the CMB is combined. Note that, for FP-DECIGO, the thick blue region completely overlaps with the green region.

takes place through the inflaton decay into the Higgs bosons and higgsinos and the reheating temperature is given by

$$T_{\rm R} \simeq 4 \times 10^8\,{\rm GeV} \left(\frac{|y|}{10^{-6}}\right) \left(\frac{m}{10^{13}\,{\rm GeV}}\right)^{1/2}. \tag{46}$$

Importantly, the smallness of the coupling constant $|y| \lesssim 10^{-6}$ is required from the successful inflaton dynamics so that the Higgs fields should not become tachyonic during inflation [42].

Finally, we comment on the particle-physics aspects to determine the reheating temperature. In supersymmetric (SUSY) theories, the abundance of the gravitino is proportional to the reheating temperature [43]:

$$\frac{n_{3/2}}{s} \sim 2 \times 10^{-12} \left(1 + \frac{m_{\tilde{g}}^2}{3m_{3/2}^2}\right) \left(\frac{T_{\rm R}}{10^{10}\,{\rm GeV}}\right), \tag{47}$$

where $n_{3/2}$ and s are the gravitino number density and the entropy density, $m_{3/2}$ ($m_{\tilde{g}}$) denotes the gravitino (gluino) mass. Hence the reheating temperature is bounded from above depending on the gravitino mass [44, 45]. It is

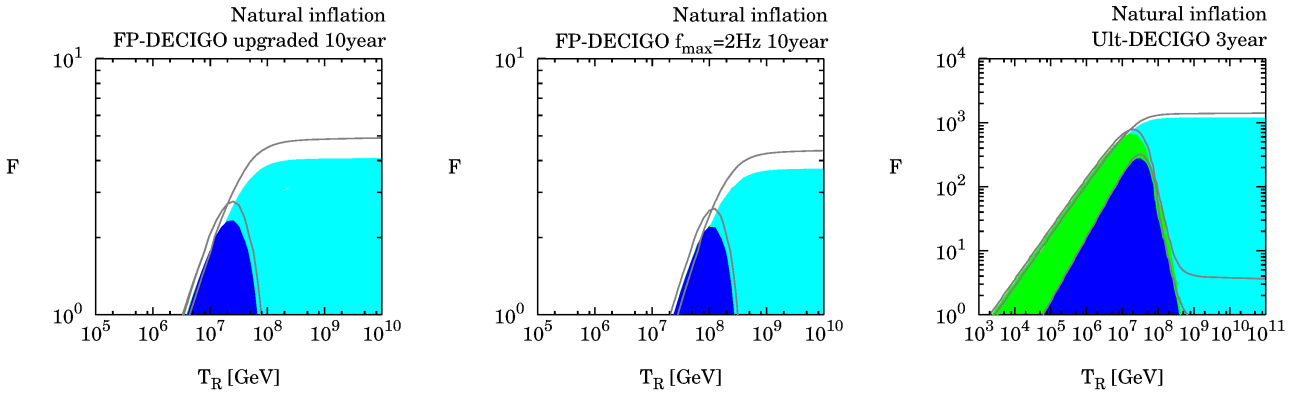

FIG. 7: The same figure for natural inflation. For comparison, the results for chaotic inflation is also plotted by gray curves.

interesting that the mass of the Higgs boson discovered at the LHC may imply relatively high scale SUSY [46–48] of $m_{3/2} \sim 100 - 1000\,\mathrm{TeV}$. In this scenario, the upper bound on T_R reads $T_\mathrm{R} \lesssim 10^9 - 10^{10}\,\mathrm{GeV}$ so that the Winos produced by the gravitino decay should not be overabundant.[2] This upper bound is close the sensitive range of the DECIGO as shown above. If the upgraded LHC discovers supersymmetry in near future, we will be able to obtain more useful information on the reheating temperature from these particle physics considerations. Needless to say, further observations of CMB temperature anisotropy and B-mode polarization in near future will also provide us with invaluable information on the tensor amplitude at the DECIGO band as well as to determine the model of inflation.

Hence we should watch these progress to design the specifications of DECIGO to extract maximal cosmological information, so that it can determine when the Big Bang happened.

Acknowledgments

We would like to thank Masaki Ando for providing a code to calculate the sensitivity curves, Masatake Ohashi and Atsushi Taruya for useful communications on the sensitivities of DECIGO. This work was supported in part by JSPS Grant-in-Aid for Scientific Research (A) (No.26247042 [KN]), Scientific Research (B) (No. 23340058 [JY]), Young Scientists (B) (No.26800121 [KN]) and Grant-in-Aid for Scientific Research on Innovative Areas 2603 ([KN]).

[1] K. Sato, Mon. Not. Roy. Astron. Soc. **195**, 467 (1981); A.H. Guth, Phys. Rev. **D23**, 347 (1981)
[2] A.A. Starobinsky Phys. Lett. **91B**, 99 (1980)
[3] V. F. Mukhanov and G. V. Chibisov, JETP Lett. **33**, 532 (1981) [Pisma Zh. Eksp. Teor. Fiz. **33**, 549 (1981)]; S.W. Hawking, Phys. Lett. **115B**, 295 (1982); A.A. Starobinsky, Phys. Lett. **117B**, 175 (1982); A.H. Guth and S-Y. Pi, Phys. Rev. Lett. **49**, 1110 (1982).
[4] D. N. Spergel *et al.* [WMAP Collaboration], Astrophys. J. Suppl. **148**, 175 (2003) [astro-ph/0302209]; H. V. Peiris *et al.* [WMAP Collaboration], Astrophys. J. Suppl. **148**, 213 (2003) [astro-ph/0302225].
[5] G. Hinshaw *et al.* [WMAP Collaboration], Astrophys. J. Suppl. **208**, 19 (2013) [arXiv:1212.5226 [astro-ph.CO]].
[6] P. A. R. Ade *et al.* [Planck Collaboration], arXiv:1303.5076 [astro-ph.CO].
[7] P. A. R. Ade *et al.* [Planck Collaboration], arXiv:1303.5082 [astro-ph.CO].
[8] P. A. R. Ade *et al.* [Planck Collaboration], arXiv:1303.5084 [astro-ph.CO].
[9] P. A. R. Ade *et al.* [BICEP2 Collaboration], Phys. Rev. Lett. **112**, 241101 (2014) [arXiv:1403.3985 [astro-ph.CO]].
[10] A.A. Starobinsky, JETP Lett. **30**, 682 (1979); V.A. Rubakov, M.V. Sazin, and A.V. Veryaskin, Phys. Lett. **115B**, 189(1982); L.F. Abbott and M.B. Wise, Nucl. Phys. B **244**, 541 (1984).

[2] In this mass range of the gravitino, nonthermal gravitino production from the inflaton decay is also harmless [49].

[11] J. L. Cervantes-Cota and H. Dehnen, Nucl. Phys. B **442**, 391 (1995) [astro-ph/9505069]; F. L. Bezrukov and M. Shaposhnikov, Phys. Lett. B **659**, 703 (2008) [arXiv:0710.3755 [hep-th]]; A. O. Barvinsky, A. Y. .Kamenshchik and A. A. Starobinsky, JCAP **0811**, 021 (2008) [arXiv:0809.2104 [hep-ph]].

[12] K. Kamada, T. Kobayashi, M. Yamaguchi and J. Yokoyama, Phys. Rev. D **83**, 083515 (2011) [arXiv:1012.4238 [astro-ph.CO]]. K. Kamada, T. Kobayashi, T. Kunimitsu, M. Yamaguchi and J. Yokoyama, Phys. Rev. D **88**, 123518 (2013) [arXiv:1309.7410 [hep-ph]].

[13] K. Nakayama and F. Takahashi, JCAP **1011**, 009 (2010) [arXiv:1008.2956 [hep-ph]].

[14] K. Kamada, T. Kobayashi, T. Takahashi, M. Yamaguchi and J. Yokoyama, Phys. Rev. D **86**, 023504 (2012) [arXiv:1203.4059 [hep-ph]].

[15] M. J. Mortonson and U. Seljak, JCAP10(2014)035 [arXiv:1405.5857 [astro-ph.CO]]. R. Flauger, J. C. Hill and D. N. Spergel, JCAP **1408**, 039 (2014) [arXiv:1405.7351 [astro-ph.CO]]. R. Adam *et al.* [Planck Collaboration], arXiv:1409.5738 [astro-ph.CO].

[16] N. Seto, S. Kawamura, and T. Nakamura, Phys. Rev. Lett. **87**, 221103 (2001); S. Kawamura *et al.*, Class. Quant. Grav. **23**, S125 (2006).

[17] N. Seto, J. Yokoyama, J. Phys. Soc. Jap. **72**, 3082-3086 (2003). [gr-qc/0305096]; H. Tashiro, T. Chiba, M. Sasaki, Class. Quant. Grav. **21**, 1761-1772 (2004). [gr-qc/0307068]; L. A. Boyle, P. J. Steinhardt, Phys. Rev. **D77**, 063504 (2008). [astro-ph/0512014]; K. Nakayama, S. Saito, Y. Suwa, J. Yokoyama, Phys. Rev. **D77**, 124001 (2008). [arXiv:0802.2452 [hep-ph]]; K. Nakayama, S. Saito, Y. Suwa, J. Yokoyama, JCAP **0806**, 020 (2008). [arXiv:0804.1827 [astro-ph]]; K. Nakayama, J. Yokoyama, JCAP **1001**, 010 (2010). [arXiv:0910.0715 [astro-ph.CO]].

[18] S. Kuroyanagi, K. Nakayama and S. Saito, Phys. Rev. D **84**, 123513 (2011) [arXiv:1110.4169 [astro-ph.CO]].

[19] A.D. Linde, Phys. Lett. B **129**, 177 (1983).

[20] H. Murayama, H. Suzuki, T. Yanagida and J. Yokoyama, Phys. Rev. Lett. **70**, 1912 (1993);Phys. Rev. D **50**, 2356 (1994); M. Kawasaki, M. Yamaguchi and T. Yanagida, Phys. Rev. Lett. **85**, 3572 (2000); K. Kadota and J. Yokoyama, Phys. Rev. D **73**, 043507 (2006) [hep-ph/0512221].

[21] K. Freese, J. A. Frieman and A. V. Olinto, Phys. Rev. Lett. **65**, 3233 (1990).

[22] S. Kuroyanagi and T. Takahashi, JCAP **1110**, 006 (2011) [arXiv:1106.3437 [astro-ph.CO]].

[23] S. Kuroyanagi, T. Chiba and N. Sugiyama, Phys. Rev. D **79**, 103501 (2009) [arXiv:0804.3249 [astro-ph]]; Phys. Rev. D **83**, 043514 (2011) [arXiv:1010.5246 [astro-ph.CO]].

[24] S. Kuroyanagi, S. Tsujikawa, T. Chiba and N. Sugiyama, Phys. Rev. D **90**, 063513 (2014) [arXiv:1406.1369 [astro-ph.CO]].

[25] M. S. Turner, M. J. White, J. E. Lidsey, Phys. Rev. **D48**, 4613-4622 (1993). [astro-ph/9306029].

[26] K. Nakayama, S. Saito, Y. Suwa, J. Yokoyama, JCAP **0806**, 020 (2008). [arXiv:0804.1827 [astro-ph]].

[27] R. Jinno, T. Moroi and K. Nakayama, JCAP **1401**, 040 (2014) [arXiv:1307.3010].

[28] S. Kuroyanagi, T. Takahashi and S. Yokoyama, arXiv:1407.4785 [astro-ph.CO].

[29] G. D. Coughlan, W. Fischler, E. W. Kolb, S. Raby and G. G. Ross, Phys. Lett. B **131**, 59 (1983). T. Moroi, M. Yamaguchi and T. Yanagida, Phys. Lett. B **342**, 105 (1995); M. Kawasaki, T. Moroi and T. Yanagida, Phys. Lett. B **370**, 52 (1996); S. Nakamura and M. Yamaguchi, Phys. Lett. B **655**, 167 (2007).

[30] T. Moroi and L. Randall, Nucl. Phys. B **570**, 455 (2000); K. Kohri, M. Yamaguchi and J. Yokoyama, Phys. Rev. D **70**, 043522 (2004); Phys. Rev. D **72**, 083510 (2005); M. Endo, K. Hamaguchi and F. Takahashi, Phys. Rev. Lett. **96**, 211301 (2006) [hep-ph/0602061]. M. Nagai and K. Nakayama, Phys. Rev. D **76**, 123501 (2007).

[31] N. Seto, Phys. Rev. D **73**, 063001 (2006) [gr-qc/0510067].

[32] S. Kuroyanagi, C. Gordon, J. Silk and N. Sugiyama, Phys. Rev. D **81**, 083524 (2010) [Erratum-ibid. D **82**, 069901 (2010)] [arXiv:0912.3683 [astro-ph.CO]]. S. Kuroyanagi, C. Ringeval and T. Takahashi, Phys. Rev. D **87**, 083502 (2013) [arXiv:1301.1778 [astro-ph.CO]].

[33] R. Jinno, T. Moroi and T. Takahashi, arXiv:1406.1666 [astro-ph.CO].

[34] B. Allen and J. D. Romano, Phys. Rev. D **59**, 102001 (1999) [gr-qc/9710117].

[35] A. J. Farmer and E. S. Phinney, Mon. Not. Roy. Astron. Soc. **346**, 1197 (2003) [arXiv:astro-ph/0304393].

[36] M. Maggiore, Phys. Rept. **331**, 283 (2000) [gr-qc/9909001].

[37] M. Maggiore, "Gravitational Waves Volume 1: Theory and Experiments," Oxford University Press (Oxford, 2008)

[38] S. Kawamura, M. Ando, N. Seto, S. Sato, T. Nakamura, K. Tsubono, N. Kanda and T. Tanaka *et al.*, Class. Quant. Grav. **28**, 094011 (2011).

[39] K. Yagi and N. Seto, Phys. Rev. D **83**, 044011 (2011) [arXiv:1101.3940 [astro-ph.CO]].

[40] D. H. Lyth, Phys. Rev. Lett. **78**, 1861 (1997) [hep-ph/9606387].

[41] M. Kawasaki, M. Yamaguchi and T. Yanagida, Phys. Rev. Lett. **85**, 3572 (2000) [hep-ph/0004243].

[42] K. Nakayama, F. Takahashi and T. T. Yanagida, JCAP **1308**, 038 (2013) [arXiv:1305.5099 [hep-ph]].

[43] M. Bolz, A. Brandenburg and W. Buchmuller, Nucl. Phys. B **606**, 518 (2001) [Erratum-ibid. B **790**, 336 (2008)] [hep-ph/0012052]; J. Pradler and F. D. Steffen, Phys. Rev. D **75**, 023509 (2007) [hep-ph/0608344]; Phys. Lett. B **648**, 224 (2007) [hep-ph/0612291]; V. S. Rychkov and A. Strumia, Phys. Rev. D **75**, 075011 (2007) [hep-ph/0701104].

[44] M. Kawasaki, K. Kohri and T. Moroi, Phys. Lett. B **625**, 7 (2005); Phys. Rev. D **71**, 083502 (2005).

[45] T. Moroi, H. Murayama and M. Yamaguchi, Phys. Lett. B **303**, 289 (1993); A. de Gouvea, T. Moroi and H. Murayama, Phys. Rev. D **56**, 1281 (1997).

[46] M. Ibe and T. T. Yanagida, Phys. Lett. B **709**, 374 (2012) [arXiv:1112.2462 [hep-ph]].

[47] N. Arkani-Hamed, A. Gupta, D. E. Kaplan, N. Weiner and T. Zorawski, arXiv:1212.6971 [hep-ph].

[48] A. Arvanitaki, N. Craig, S. Dimopoulos and G. Villadoro, JHEP **1302**, 126 (2013) [arXiv:1210.0555 [hep-ph]].

[49] K. Nakayama, F. Takahashi and T. T. Yanagida, Phys. Lett. B **734**, 358 (2014) [arXiv:1404.2472 [hep-ph]].